JOURNAL OF PROPULSION AND POWER
Vol. 21, No. 6, November–December 2005

# Time-Averaged Entropy and Total Pressure Ratios Across Unsteady Inlet Shock Waves

Mark J. Lewis* and Kerrie A. Smith†
*University of Maryland, College Park, Maryland 20742-3015*

**Unsteady shock-wave motion can have a significant effect on the flow in a supersonic inlet, or in a compressor or turbine passage. One particular consequence of unsteadiness is that the time average of moving shock-wave properties can be noticeably different than the corresponding values for a steady shock. Of special interest to propulsion applications, shock unsteadiness can either increase or decrease the time-averaged total pressure ratio in the shock reference frame and the time average of frame-independent entropy jump, depending on the shock-normal Mach number. However, unsteadiness will always lead to a decrease in time-averaged total pressure ratio in the absolute frame and thus downstream of the unsteady shock. An analysis is presented, which includes time averaging of the sinusoidally perturbed, quasi-steady Rankine–Hugoniot equations, from which the time-dependent responses are calculated using both a differential and integral approach. Functions are derived that permit the direct calculation of time-averaged unsteady losses in total pressure and increase in entropy, assuming sinusoidal perturbation. Both computational and analytical studies have been performed to quantify the conditions under which the shock entropy jump will either increase or decrease as a result of periodic unsteadiness.**

## Nomenclature

| | | |
|---|---|---|
| $M$ | = | Mach number |
| $P$ | = | pressure, Pa |
| $R$ | = | gas constant for air, 287 J/kg-K |
| $s$ | = | entropy, J/kg-K |
| $T$ | = | temperature, K |
| $\beta$ | = | shock-wave angle |
| $\gamma$ | = | ratio of specific heats |
| $\Delta$ | = | shock jump value |
| $\varepsilon$ | = | ratio of perturbed value to steady state |
| $\theta$ | = | oblique surface angle |
| $\mu$ | = | Mach number perturbation amplitude |
| $\rho$ | = | density, kg/m$^3$ |
| $\phi$ | = | pressure perturbation amplitude |

*Subscripts*

| | | |
|---|---|---|
| 0 | = | total conditions |
| 1 | = | upstream value |
| 2 | = | downstream value |
| $\infty$ | = | freestream conditions |

## I. Introduction

A FAMILIAR property of the standard Rankine–Hugoniot equations is the essential nonlinearity of the shock jump conditions. It is well known that standard thermodynamic changes across the shock, including static pressure, temperature, and density, are all nonlinear in Mach number. Similarly, it can be shown that the increase in entropy $\Delta s$ across a shock wave is also nonlinear; for instance, $\Delta s$ is proportional to $(M_\infty^2 - 1)^3$ near Mach 1 (Ref. 1). This nonlinearity has an interesting effect on the time average of total pressure and entropy across a periodically moving quasi-steady shock wave, as might be encountered in a supersonic or hypersonic inlet, or in a transonic compressor or turbine passage. Ng and Epstein first identified this, and the resulting entropy-related consequences as an important issue in transonic compressor passage flows, pointing out the unique properties of unsteady flow compared to the steady-state behavior.[2] The mechanisms that generate and the conditions that favor such oscillatory flows have been an important subject of research in a number of fields. Transonic diffusers are also prone to unsteadiness, as a result of combustion instabilities.[3–6] The stability of the strong and weak solutions to supersonic flow over a wedge has been studied via perturbation analysis,[7–10] as well as methods of computationally treating oblique shock oscillation.[11,12] Finally, inlets of pulse detonation engines are prone to unsteady flows because of the periodic nature of the detonations.[13–16] A primary concern connected with shock motion in inlets is that it can lead to engine unstart, but in the present work it shall be shown that unsteadiness might have other consequences as well.

As an example, Fig. 1 presents the time history of the entropy jump across a shock that is oscillating about a steady-state normal Mach number of 1.5, in order to produce a $\pm 10\%$ variation in static pressure. Note that the entropy increase in the first part of the cycle, when static pressure is higher and the shock is moving into the approaching flow, is larger in magnitude than the entropy decrease in the second part of the cycle, when static pressure is decreased and the shock is moving away from the incoming flow. The net result of this is that the time-averaged entropy jump over one complete cycle is larger than the entropy jump for a shock wave fixed at the steady-state Mach 1.5 condition.

In contrast, Fig. 2 presents the entropy jump across a shock wave oscillating about normal Mach 3, again to produce a $\pm 10\%$ variation in static pressure. At this time-averaged Mach number, the time average of the entropy jump is smaller than that of the jump across a shock, which is fixed at the steady-state point. In other words, an oscillating shock wave can yield either higher or lower time-averaged entropy changes, depending on the steady-state value of the Mach number. This phenomenon can be understood from either numerical simulation or analytical solution, as will be shown next.

This result can raise some interesting questions based on the principle of minimum entropy production, which Li and Ben-Dor have used to explain plausible shock solutions when multiple solutions are available.[17,18] This principle postulates that, given several possible solutions, the one which results in the minimum positive entropy rise will be the one that is observed, though the reliability of this principle in determining the behavior of real devices is still unproved. In fact there is significant disagreement with the applicability of this principle in selecting shock solutions,[9] and so any conclusions

Received 5 October 2004; revision received 24 March 2005; accepted for publication 24 March 2005. 

*Chief Scientist of the Air Force, Department of Aerospace Engineering. Fellow AIAA.

†Graduate Assistant, Department of Aerospace Engineering. Student Member AIAA.

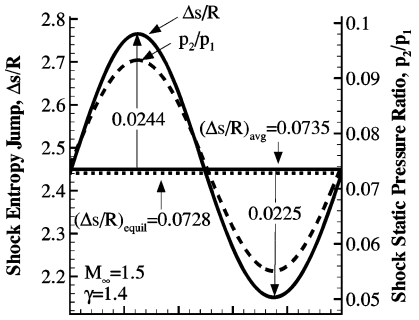


**Fig. 1 Shock entropy rise driven by sinusoidal static-pressure rise, with upstream Mach number 1.5. Entropy increase early in the cycle ($0 - \pi$) is greater in magnitude than the entropy decrease later in the cycle ($\pi - 2\pi$).**

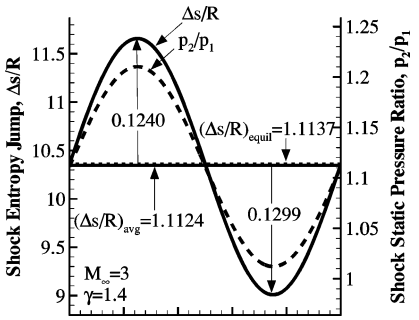


**Fig. 2 Shock entropy rise driven by sinusoidal static pressure rise, with upstream Mach number 3. Entropy increase early in the cycle ($0 - \pi$) is smaller in magnitude than the entropy decrease later in the cycle ($\pi - 2\pi$).**

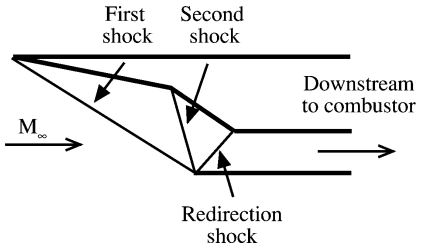


**Fig. 3 Typical two-ramp inlet.**

derived from this reasoning would be highly speculative. If applicable, minimum entropy production suggests that a time-averaged phenomenon which decreases entropy rise across the shock wave should be more likely than one which increases entropy, assuming that boundary conditions will permit both solutions. This in turn could impact the overall behavior of an inlet, including its delivery conditions. For instance, shock interactions can be extremely sensitive to shock motion, and inherent unsteadiness could be a factor in cowl-shock matching.[19,20] Entropy considerations do not cause unsteadiness in and of themselves; some mechanism for the physical onset of unsteadiness, such as an aeroelastic structural deflection of the vehicle, atmospheric nonuniformity, or combustion instability is required. If the principle of minimum entropy production is applicable, it can at most suggest a "preferred" solution. This result will remain an unproven speculation in the present work, until the applicability of the principle can either be established or disproven.

Inlet shock systems can be rather complex, with multiple oblique, or even three-dimensional shocks. A typical, two-ramp scramjet inlet is shown in Fig. 3. This inlet would be attached to some vehicle traveling at a freestream Mach number of $M_\infty$. A series of oblique shocks serve to slow and compress the flow to supply the correct downstream conditions to the combustor. Such an inlet is designed so that all of the shocks will intersect the lip of the cowl. If the flow is perturbed from its design conditions, such as when the vehicle changes angle of attack, turns, or travels through nonuniformities in the atmosphere, the shock angles can change. If the shock angle increases so that shock moves outside of the cowl, spillage occurs, and the vehicle experiences increased drag and lowered efficiency. If the shock angle decreases so that the shock moves inside the cowl, shock-boundary-layer interactions can cause intense localized heating and flow separation. Changes in upstream conditions at the mouth of the inlet can result in dramatic changes in the quality of the flow supplied downstream to the combustor. Because of the complex geometry of such an inlet and the number of parameters involved, it would be difficult to examine the effects of unsteadiness the entire system. However, it is well known that across a single shock the essential physics of the jump properties are governed only by the local normal Mach number. As such, we consider the simplest case of unsteadiness across a normal shock wave. The total pressure jump across a normal shock wave, as a function of upstream Mach number, is given by the familiar expression:

$$\frac{p_{0,2}}{p_{0,1}} = \left[1 + \frac{2\gamma}{\gamma+1}\left(M_1^2 - 1\right)\right]^{-1/(\gamma-1)} \left[\frac{(\gamma-1)M_1^2 + 2}{(\gamma+1)M_1^2}\right]^{-\gamma/(\gamma-1)} \tag{1}$$

Under the quasi-steady assumption, this will be applied to the oscillating shock wave at each point in its cycle, such as a shock wave moving in an inlet duct. In the frame of reference of the shock wave and, in the absence of heat addition, total temperature is constant, so that $\Delta s = -R\,\ell n(p_{0,2}/p_{0,1})$. The entropy jump across the shock wave is then directly related to the total pressure jump in the shock reference frame:

$$\frac{\Delta s}{R} = \ell n \left\{ \left[1 + \frac{2\gamma}{\gamma+1}\left(M_1^2 - 1\right)\right]^{1/(\gamma-1)} \left[\frac{(\gamma-1)M_1^2 + 2}{(\gamma+1)M_1^2}\right]^{\gamma/(\gamma-1)} \right\} \tag{2}$$

Because entropy is a state variable, this is frame independent.

Of particular interest for various practical applications, including propulsion systems, is the change in total pressure and entropy as a function of the change in static-pressure ratio. The static-pressure ratio might be changing as a result of either upstream or downstream pressure changes. Of particular interest might be unsteady downstream static-pressure changes caused by combustor instabilities, propagating upstream to the inlet. In a flow that is supersonic everywhere along a given direction, downstream disturbances are unable to propagate upstream because their propagation speed is less than the speed of the flow. However, disturbances can be admitted through boundaries of a supersonic region. Consider a normal shock in steady flow. The pressure ratio across the shock can be calculated as a function of upstream Mach number. Without changing the freestream velocity, suppose a brief increase in pressure is imposed downstream of the shock, such that the flow is now unsteady. Because the flow across a normal shock is always subsonic, this disturbance can propagate upstream until it reaches the shock. This will generate an imbalance of forces across the shock, and the shock will be pushed upstream. However, now the shock has a velocity relative to the upstream velocity, so that the shock strength will decrease, and the system will equalize. However, as soon as the downstream pressure increase is over, there will be another imbalance, and the shock will return to its previous position. Conversely, if downstream pressure is decreased, the shock will move downstream. Inducing a continuous unsteady downstream pressure oscillation will cause the shock to translate back and forth.[21] The properties of the shock will change with the imposed pressure ratio across it. The total pressure ratio and entropy jump in terms of static-pressure ratio are

$$\frac{p_{0,2}}{p_{0,1}} = \left[\frac{p_2}{p_1}\right]^{-1/(\gamma-1)} \left[\frac{(\gamma+1)[p_2/p_1] + (\gamma-1)}{(\gamma-1)[p_2/p_1] + (\gamma+1)}\right]^{\gamma/(\gamma-1)}$$

$$\frac{\Delta s}{R} = \ell n \left\{ \left[\frac{p_2}{p_1}\right]^{1/(\gamma-1)} \left[\frac{(\gamma-1)[p_2/p_1] + (\gamma+1)}{(\gamma+1)[p_2/p_1] + (\gamma-1)}\right]^{\gamma/(\gamma-1)} \right\} \tag{3}$$

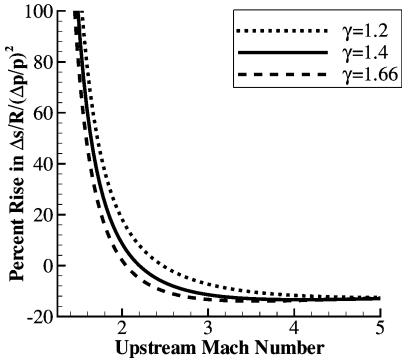


**Fig. 4 Time-averaged entropy change across a moving shock driven with sinusoidal downstream static-pressure fluctuations, as a function of the freestream Mach. Note scaling with the square of the relative disturbance amplitude.**

In this scenario the downstream perturbations can be experienced as pressure variations that the shock must accommodate. Pressure variations would cause the shock to oscillate. Because of the nonlinearity, these pressure variations would also change the freestream Mach number "seen" by the shock. Figure 4 shows the net gain or loss in entropy jump as a function of the upstream Mach number, in the laboratory frame of reference. The information has been presented in this manner so that one can imagine applying the results to a vehicle traveling at a given freestream Mach number. This also means that the shock will have a net velocity in this frame of reference. This is actually an important implication because shock location is usually an important parameter in hypersonic vehicle design. If the shock moves toward the front of the vehicle, it could lead to spillage and additional drag, or engine unstart. If it moves in the opposite direction, into the cowl, shock-boundary-layer interactions could occur, causing intense localized heating. Note again that for small supersonic Mach number a cyclical unsteadiness will increase overall entropy jump, but for high Mach numbers the unsteadiness decreases the overall entropy jump.

## II. Analytical Solutions for Time-Averaged Properties

### A. Changes Caused by Mach-Number Variation

*1. Shock-Frame Total Pressure*

A closed-form solution can be obtained for the magnitude and Mach-number dependence of time-averaged total pressure and entropy across a moving shock wave, subject to a sinusoidal oscillation in either normal Mach number or downstream static pressure. Mach number is separated into a steady-state component $\hat{M}$, and a time-varying portion $M'$ that represents a shock with some steady-state upstream Mach number and an imposed perturbation. In this paper, a sinusoidal perturbation has been chosen so that the solution can be integrated, but a sawtooth, square wave or other waveform would be equally appropriate. Assuming quasi-steady behavior, such that at any moment the shock properties are a function of the instantaneous upstream boundary conditions in the shock frame of reference, the time-averaged quasi-steady total pressure ratio (in the shock frame of reference) and entropy change are

$$\left.\frac{\overline{p_{02}}}{p_{01}}\right|_{\substack{\text{unsteady}\\ \text{Mach}}} = \frac{1}{T}\int_0^T \left[\left(1+\frac{2\gamma}{\gamma+1}\{[\hat{M}+M'(t)]^2-1\}\right)^{-1/(\gamma-1)} \times \left\{\frac{(\gamma+1)[\hat{M}+M'(t)]^2}{(\gamma-1)[\hat{M}+M'(t)]^2+2}\right\}^{\gamma/(\gamma-1)}\right] \mathrm{d}t$$

$$\left.\frac{\overline{\Delta s}}{R}\right|_{\substack{\text{unsteady}\\ \text{Mach}}} = \frac{1}{T}\int_0^T \ell_n\left[\left(1+\frac{2\gamma}{\gamma+1}\{[\hat{M}+M'(t)]^2-1\}\right)^{1/(\gamma-1)} \times \left\{\frac{(\gamma+1)[\hat{M}+M'(t)]^2+2}{(\gamma-1)[\hat{M}+M'(t)]^2}\right\}^{-\gamma/(\gamma-1)}\right] \mathrm{d}t \tag{4}$$

Writing the amplitude of the time-varying component of normal Mach number as a fraction $\varepsilon$ of the steady-state value, the argument of the integral for time-averaged total pressure ratio is

$$\begin{aligned}&\left[1+\frac{2\gamma}{\gamma+1}(\{\hat{M}[1+\varepsilon(t)]\}^2-1)\right]^{-1/(\gamma-1)} \times\left(\frac{(\gamma+1)\{\hat{M}[1+\varepsilon(t)]\}^2}{(\lambda-1)\{\hat{M}[1+\varepsilon(t)]\}^2+2}\right)^{\gamma/(\gamma-1)}\\ &=\left[1+\frac{2\gamma}{\gamma+1}(\hat{M}^2-1)\right]^{-1/(\gamma-1)}\left[\frac{(\gamma+1)\hat{M}^2}{(\lambda-1)\hat{M}^2+2}\right]^{\gamma/(\gamma-1)} \times\left[1+\frac{2\gamma\hat{M}^2(2\varepsilon+\varepsilon^2)}{2\gamma\hat{M}^2-(\gamma-1)}\right]^{-1/(\gamma-1)}[1+2\varepsilon+\varepsilon^2]^{\gamma/(\gamma-1)}\\ &\times\left[1+\frac{(\gamma-1)\hat{M}^2(2\varepsilon+\varepsilon^2)}{(\gamma-1)\hat{M}^2+2}\right]^{-\gamma/(\gamma-1)}\end{aligned} \tag{5}$$

The time-varying Mach-number term can be expanded, but it is necessary to retain the nonlinear behavior to explore the phenomena of interest in this present work, that is, if only first-order terms in $\varepsilon$ are retained, the variations in shock properties must average to the steady-state values. Based on the binomial expansion, the following substitutions are used:

$$\begin{aligned}(1+a\varepsilon)^n &\cong 1+na\varepsilon+n(n-1)a^2\varepsilon^2/2\\ (1+a[2\varepsilon+\varepsilon^2])^n &\cong 1+1na\varepsilon+na(1+2a[n-1])\varepsilon\end{aligned} \tag{6}$$

where we assume that $a\varepsilon \ll 1$. The perturbation in Mach number is written as a sinusoid, such that $\varepsilon = \mu \sin \omega t$. Integrating Eq. (5) through one cycle ($0 \le t \le 2\pi/\omega$) using the expansion of Eq. (6), the first-order $\varepsilon$ terms integrate to zero; neglecting all terms in $\varepsilon^3$ or higher, only the $\varepsilon^2$ terms remain. As a result, the time-averaged total pressure ratio can be written as the steady-state value plus a nonlinear function of the ratio of specific heats $\gamma$ and upstream normal Mach number $M_1$.

$$\begin{aligned}\left.\frac{p_{0,2}}{p_{0,1}}\right|_{\text{avg}} &\cong \left.\frac{p_{0,2}}{p_{0,1}}\right|_{\text{eq.}}\left\{1+\frac{2\gamma(\gamma+1)\left(M_1^2-1\right)\left(2\gamma M_1^6-[9\gamma-1]M_1^4+3[\gamma-1]M_1^2-2\right)}{\left[\left([\gamma-1]M_1^2+2\right)\left(2\gamma M_1^2-[\gamma-1]\right)\right]^2}\frac{\int_0^{2\pi}\mu^2\sin^2\theta\,\mathrm{d}\theta}{2\pi}\right\}\\ &= \left.\frac{p_{0,2}}{p_{0,1}}\right|_{\text{eq.}}\left\{1+\frac{\gamma(\gamma+1)\left(M_1^2-1\right)\left(2\gamma M_1^6-[9\gamma-1]M_1^4+3[\gamma-1]M_1^2-2\right)}{\left[\left([\gamma-1]M_1^2+2\right)\left(2\gamma M_1^2-[\gamma-1]\right)\right]^2}\mu^2\right\}\\ &\equiv \left.\frac{p_{0,2}}{p_{0,1}}\right|_{\text{eq.}}\left\{1+F_{p_{0,M}}\mu^2\right\}\end{aligned} \tag{7}$$

at $\gamma = 1.4$ (or 7/5)

$$F_{p_0,M} = \frac{105\left(M_1^2-1\right)\left(7M_1^6-29M_1^4+3M_1^2-5\right)}{98M_1^8+952M_1^6+2172M_1^4-680M_1^2+50}$$
$$= \frac{\left(M_1^2-1\right)\left(7.5M_1^6-31.0714M_1^4+3.2143M_1^2-5.357\right)}{M_1^8+9.7143M_1^6+22.1633M_1^4-6.9388M_1^2+0.5102} \tag{8}$$

As defined, $F_{p_0,M}$ is proportional to the fractional added total pressure that results from the oscillation, normalized to the upstream value. The numerator of the second term in Eq. (7) has a zero when $2\gamma M_1^6-[9\gamma-1]M_1^4+3[\gamma-1]M_1^2=2$. At this point, $F_{p_0,M}=0$, which occurs at $M_1=2.020$ for $\gamma=1.4$. Thus, for a shock in air with normal Mach 2.020, a small oscillation neither increases nor decreases the time-averaged downstream total pressure in the shock frame of reference. Below that Mach number, $F_{p_0,M}$ is negative, and the total pressure ratio across the oscillating shock wave, in the shock frame of reference, is less than that of the steady-state value. Note also that the change in total pressure ratio caused by the unsteadiness is proportional to the square of the Mach-number amplitude variation, a result that has been confirmed numerically.

*2. Entropy Rise*

Following a similar derivation to that of the total pressure change, the entropy jump across a moving shock wave is determined as a function of varying normal Mach number, for small perturbations from a steady-state value. Note that unlike total pressure ratio, the entropy jump is a change in state variable, and so is independent of the frame of reference. With time-dependent Mach number, the right-hand side of Eq. (2) is written:

$$\ell_n\left[1+\frac{2\gamma}{\gamma+1}\left(\{\hat{M}[1+\varepsilon(t)]\}^2-1\right)\right]^{1/(\gamma-1)} \times\left(\frac{(\gamma+1)\{\hat{M}[1+\varepsilon(t)]\}^2+2}{(\lambda-1)\{\hat{M}[1+\varepsilon(t)]\}^2}\right)^{\gamma/(\gamma-1)}$$
$$= \ell_n\left[1+\frac{2\gamma}{\gamma+1}(\hat{M}^2-1)\right]^{1/(\gamma-1)}\left[\frac{(\gamma+1)\hat{M}^2}{(\gamma-1)\hat{M}^2+2}\right]^{\gamma/(\gamma-1)}$$
$$+\frac{1}{\gamma-1}\ell_n\left[1+\frac{2\gamma\hat{M}^2(2\varepsilon+\varepsilon^2)}{2\gamma\hat{M}^2-(\gamma-1)}\right]$$
$$-\frac{\gamma}{\gamma-1}\ell_n[1+2\varepsilon+\varepsilon^2]$$
$$+\frac{\gamma}{\gamma-1}\ell_n\left[1+\frac{(\gamma-1)\hat{M}^2(2\varepsilon+\varepsilon^2)}{(\gamma-1)\hat{M}^2+2}\right]^{-\gamma/(\gamma-1)} \tag{9}$$

In a manner analogous to using the expansion of Eq. (6) to represent the perturbation, the time-averaged entropy rise across the shock can be found by approximating $\ell_n(1+x)\cong x-\frac{1}{2}x^2$, from the Taylor-series expansion of the natural logarithm function. Also as before, the terms that are first order in $\varepsilon$ will integrate to zero over one sinusoidal cycle, and neglecting all terms in $\varepsilon^3$ or higher only terms in $\varepsilon^2$ will remain.

Equation (9) can then be written in the following approximate form:

$$\ell_n\left[1+\frac{2\gamma}{\gamma+1}\left(\{\hat{M}[1+\varepsilon(t)]\}^2-1\right)\right]^{1/(\gamma-1)} \times\left(\frac{(\gamma+1)\{\hat{M}[1+\varepsilon(t)]\}^2+2}{(\lambda-1)\{\hat{M}[1+\varepsilon(t)]\}^2}\right)^{\gamma/(\gamma-1)}$$
$$\cong \ell_n\left[1+\frac{2\gamma}{\gamma+1}(\hat{M}^2-1)\right]^{1/(\gamma-1)}\left[\frac{(\gamma+1)\hat{M}^2}{(\gamma-1)\hat{M}^2+2}\right]^{\gamma/(\gamma-1)}$$
$$+\frac{4\gamma\left(M_1^2-1\right)^2\varepsilon}{\left([\gamma-1]M_1^2+2\right)\left(2\gamma M_1^2-[\gamma-1]\right)}-\varepsilon^2\left(M_1^2-1\right)$$
$$\times\frac{2[\gamma-1]\left(\gamma M_1^6+1\right)-[9\gamma^2-4\gamma-1]M_1^4+3[\gamma^2-4\gamma-1]M_1^2}{2\gamma\left[\left([\gamma-1]M_1^2+2\right)\left(2\gamma M_1^2-[\gamma-1]\right)\right]^2} \tag{10}$$

Setting $\varepsilon=\mu\sin\omega t$ and integrating through one cycle, through which the first-order $\varepsilon$ term once again integrates to zero (leaving higher-order terms in $\varepsilon$),

$$\left.\frac{\Delta s}{R}\right|_{\text{avg}} = \left.\frac{\Delta s}{R}\right|_{\text{equil}}$$
$$-\left\{\frac{2[\gamma-1]\left(\gamma M_1^6+1\right)-[9\gamma^2-4\gamma-1]M_1^4+3[\gamma^2-4\gamma-1]M_1^2}{\left[\left([\gamma-1]M_1^2+2\right)\left(2\gamma M_1^2-[\gamma-1]\right)\right]^2}2\gamma\left(M_1^2-1\right)\frac{\int_0^{2\pi}\mu^2\sin^2(\theta)\,\mathrm{d}\theta}{2\pi}\right\}$$
$$= \left.\frac{\Delta s}{R}\right|_{\text{equil}}-\frac{2[\gamma-1]\left(\gamma M_1^6+1\right)-[9\gamma^2-4\gamma-1]M_1^4+3[\gamma^2-4\gamma-1]M_1^2}{\left[\left([\gamma-1]M_1^2+2\right)\left(2\gamma M_1^2[\gamma-1]\right)\right]^2}\left(M_1^2-1\right)\gamma\mu^2$$
$$= \left.\frac{\Delta s}{R}\right|_{\text{equil}}+G_{\Delta s,M}\mu^2 \tag{11}$$

where the steady-state value of $\Delta s/R$ is the value at the steady-state pressure. At $\gamma=7/5$,

$$G_{\Delta s,M} = \frac{-1.25M_1^8+13.5715M_1^6+3.2143M_1^4-16.4286M_1^2+0.8929}{M_1^8+9.7143M_1^6+22.1633M_1^4-6.9388M_1^2+0.5102}$$
$$= \frac{-245M_1^8+2660M_1^6+630M_1^4-3220M_1^2+175}{196M_1^8+1904M_1^6+4344M_1^4-1360M_1^2+100} \tag{12}$$

This also has a zero value, $G_{\Delta s,M}=0$ at $M_1=3.314$ for $\gamma=1.4$. Below that Mach number, $G_{\Delta s,M}$ is positive, and a periodically oscillating shock has more entropy rise than the steady-state shock wave. Note that the zero values for entropy and total pressure occur at different normal steady-state Mach numbers.

### B. Changes Caused by Static-Pressure Variation

*1. Shock-Frame Total Pressure*

The effect of unsteady downstream static pressure on the shock total pressure and entropy is of particular interest for application to unsteady shock waves on engine inlets and in compressor passages.

With the pressure ratio $P \equiv p_2/p_1$ separated into steady and unsteady parts, as $P'(t) = \hat{P} \cdot \varepsilon(t)$, the time-averaged shock-referenced total pressure ratio and entropy rise are

$$\left.\frac{\overline{p_{02}}}{p_{01}}\right|_{\substack{\text{unsteady}\\ \text{pressure}}} = \frac{1}{T}\int_0^T \left( [\hat{P} + P'(t)]^{-1/(\gamma-1)} \left\{ \frac{(\gamma+1)[\hat{P}+P'(t)]^2 + (\gamma-1)}{(\gamma-1)[\hat{P}+P'(t)]^2 + (\gamma+1)} \right\}^{\gamma/(\gamma-1)} \right) \mathrm{d}t$$

$$\left.\frac{\overline{\Delta s}}{R}\right|_{\substack{\text{unsteady}\\ \text{Mach}}} = \frac{1}{T}\int_0^T \ell_n \left( [\hat{P} + P'(t)]^{1/(\gamma-1)} \left\{ \frac{(\gamma-1)[\hat{P}+P'(t)]^2 + (\gamma+1)}{(\gamma+1)[\hat{P}+P'(t)]^2 + (\gamma-1)} \right\}^{\gamma/(\gamma-1)} \right) \mathrm{d}t \tag{13}$$

The logarithmic derivatives of static pressure ratio and upstream Mach number across the shock are related as

$$\frac{\mathrm{d}P}{P} = \left[ \frac{4\gamma M_1^2}{2\gamma M_1^2 - (\gamma+1)} \right] \frac{\mathrm{d}M_1}{M_1} \tag{14}$$

where the term in brackets, representing the "influence" of Mach-number changes on downstream static pressure, is plotted in Fig. 5. Note that this function is approximately equal to 2 for nearly any Mach number or value of $\gamma$ of interest. Thus, for small perturbations, $P'/\hat{P} \cong 2M_1'/\hat{M}_1$, meaning that a small fractional fluctuation in Mach number corresponds to a small fractional fluctuation in static pressure. As such, the Mach number and pressure variations have similar qualitative effects on entropy and total pressure rise.

To examine the nonlinear behavior of the shock relations caused by downstream pressure variations, a similar procedure to the one described for sensitivity to Mach-number changes is followed. Writing static-pressure ratio $P'(t) = \hat{P} \cdot \varepsilon(t)$, and again using a binomial expansion out to the first nonlinear term, such that $(1+\varepsilon)^n \cong 1 + n\varepsilon + (n/2)(n-1)\varepsilon^2$, the time-dependent total pressure ratio is

$$[\hat{P}(1+\varepsilon(t))]^{-1/(\gamma-1)} \left\{ \frac{(\gamma+1)[\hat{P}(1+\varepsilon)] + (\gamma-1)}{(\gamma-1)[\hat{P}(1+\varepsilon)] + (\gamma+1)} \right\}^{\gamma/(\gamma-1)}$$

$$\cong \hat{P}^{-1/(\gamma-1)} \left[ \frac{(\gamma+1)\hat{P} + (\gamma-1)}{(\gamma-1)\hat{P} + (\gamma+1)} \right]^{\gamma/(\gamma-1)} \left[ 1 + \frac{\gamma(\gamma+1)\hat{P}\varepsilon}{[\gamma-1]^2 + [\gamma^2-1]\hat{P}} + \frac{\gamma(\gamma+1)^2\hat{P}^2\varepsilon^2}{2([\gamma-1]^2 + [\gamma^2-1]\hat{P})^2} \right]$$

$$\times \left[ 1 + \frac{\varepsilon}{\gamma-1} + \frac{\gamma\varepsilon^2}{2(\gamma-1)^2} \right] \left\{ 1 - \frac{\gamma\hat{P}\varepsilon}{(\gamma+1) + \hat{P}(\gamma-1)} + \frac{\gamma(2\gamma-1)\hat{P}^2\varepsilon^2}{2[(\gamma-1) + (\gamma+1)\hat{P}]^2} \right\} \tag{15}$$

Setting $\varepsilon = \phi \sin\omega t$ and integrating through one cycle, through which the $\varepsilon$ term integrates to zero, and neglecting all terms in $\varepsilon^3$ or higher, we obtain an expression that relates the time-averaged change in entropy jump caused by pressure variations that is very similar to Eq. (7), which related the time-averaged change in entropy jump caused by upstream Mach-number variations:

$$\left.\frac{p_{02}}{p_{01}}\right|_{\text{avg}} \cong \left.\frac{p_{02}}{p_{01}}\right|_{\text{eq.}} \left\{ 1 + \frac{\gamma[\gamma+1](\hat{P}-1)[[\gamma+1](\hat{P}^3 - 3\hat{P}^2 + 1) - [5\gamma-3]\hat{P}]}{4[[\gamma^2-1](P^2+1) + 2[\gamma^2+1]P]^2} \frac{\int_0^{2\pi} \phi^2 \sin^2(\theta)\,\mathrm{d}\theta}{2\pi} \right\}$$

$$= \left.\frac{p_{02}}{p_{01}}\right|_{\text{eq.}} \left\{ 1 + \frac{\gamma[\gamma+1](\hat{P}-1)[[\gamma+1](\hat{P}^3 - 3\hat{P}^2 - 1) - [5\gamma-3]\hat{P}]}{4[[\gamma^2-1](P^2+1) + 2[\gamma^2+1]P]^2} \phi^2 \right\}$$

$$= \left.\frac{p_{02}}{p_{01}}\right|_{\text{eq.}} \left\{ 1 + \frac{\left(M_1^2-1\right)\left(\gamma^2 M_1^6 - 3\gamma^2 M_1^4 + \gamma[\gamma-2]M_1^2 - 1\right)}{4\gamma M_1^4 \left([\gamma-1]M_1^2 + 2\right)^2} \phi^2 \right\}$$

$$= \left.\frac{p_{02}}{p_{01}}\right|_{\text{eq.}} \left\{ 1 + F_{p_0,P}\phi^2 \right\} \tag{16}$$

at $\gamma = 1.4$ (or 7/5)

$$F_{p_0,P} = \frac{315(\hat{P}^4+1) - 1260\hat{P}^3 + 420\hat{P}^2 + 210\hat{P}}{144(\hat{P}^4+1) + 1776(\hat{P}^3+\hat{P}) + 5764\hat{P}^2}$$

$$= \frac{2.1875(\hat{P}^4+1) - 8.75\hat{P}^3 + 2.9167\hat{P}^2 + 1.4583\hat{P}}{\hat{P}^4 + 12.3333(\hat{P}^3+\hat{P}) + 40.0278\hat{P}^2 + 1}$$

$$= \frac{245M_1^8 - 980M_1^6 + 630M_1^4 - 20M_1^2 + 125}{112M_1^8 + 1120M_1^6 + 2800M_1^4}$$

$$= \frac{2.1875M_1^8 - 8.75M_1^6 + 5.625M_1^6 - 0.1786M_1^2 + 1.1161}{M_1^8 + 10M_1^6 + 25M_1^4} \tag{17}$$

Note that at $\gamma = 1.4$, $F_{p_0,p} = 0$ at $M_1 = 1.785$. Below that Mach number, $F_{p_0,p} = 0$ is negative, and the total pressure across the oscillating shock wave, in the shock frame of reference, is less than that of the steady-state value.

*2. Entropy Rise*

The time-averaged entropy rise across the shock subject to pressure fluctuations can be found by once again using the approximate expansion $\ell_n(1+x) \cong x - x^2/2$ and solving for the entropy expression in Eq. (3) subject to a variation in $P = p_2/p_1$:

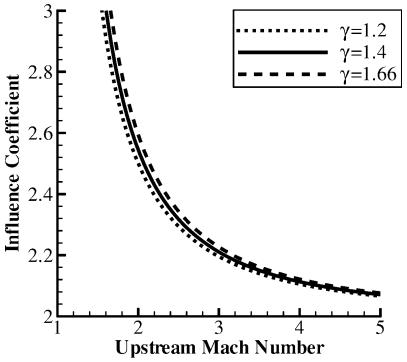


**Fig. 5 Influence coefficient representing the ratio of fractional static-pressure change to fractional upstream Mach-number change, as a function of upstream Mach number and $\gamma$.**

### C. Differential-Based Solutions

In the preceding section, the time-averaged changes in shock entropy properties were determined by integrating through a sinusoidal disturbance. Another way to view this same problem is from a differential perspective: a net gain in overall entropy occurs from oscillation when more entropy is gained by a differential increase in Mach number than is lost from a differential decrease. The critical Mach number will be found at the point where an infinitesimal increase yields the same change in entropy as an infinitesimal decrease, that is, the inflection point. Once again, note that total pressure is frame dependent, so that a gain or loss in the shock frame of reference might not correspond to a gain in the absolute frame of reference.

Figure 6 presents a plot of total pressure ratio in the shock frame of reference and the derivative of that quantity with respect to Mach number, as well as the entropy jump across the shock wave and the derivative of entropy jump with respect to Mach number for $\gamma = 1.4$. Note that both the total pressure curve and the entropy jump curve

$$
\begin{aligned}
&\ell_n\left([\hat{P}(1+\varepsilon)]^{1/(\gamma-1)}\left\{\frac{(\gamma-1)[\hat{P}(1+\varepsilon)]+(\gamma+1)}{(\gamma+1)[\hat{P}(1+\varepsilon)]+(\gamma-1)}\right\}^{\gamma/(\gamma-1)}\right)\\
&\quad\cong \ell_n\left\{\hat{P}^{1/(\gamma-1)}\left[\frac{(\gamma-1)[\hat{P}+(\gamma+1)}{(\gamma+1)\hat{P}+(\gamma-1)}\right]^{\gamma/(\gamma-1)}\right\}+\frac{\varepsilon}{\gamma-1}\left\{1-\frac{4\gamma^2\hat{P}}{[\gamma^2-1]\hat{P}^2+2[\gamma^2+1]\hat{P}+[\gamma^2-1]}\right\}\\
&\quad-\frac{\varepsilon^2}{2(\gamma-1)}\left[1-\frac{8\gamma^2([\gamma^2-1]\hat{P}^3+[\gamma^2+1]\hat{P}^2)}{[\gamma^4-2\gamma^2+1](\hat{P}^4+1)+4[\gamma^4-1](\hat{P}^3+\hat{P})+[6\gamma^4+4\gamma^2+6]\hat{P}^2}\right]
\end{aligned}
\tag{18}
$$

setting $\varepsilon = \phi \sin \omega t$ and integrating through one period:

$$
\begin{aligned}
\left.\frac{\Delta s}{R}\right|_{\text{avg}} &= \left.\frac{\Delta s}{R}\right|_{\text{eq.}}+\left[\frac{8\gamma^2([\gamma^2-1]\hat{P}^3+[\gamma^2+1]\hat{P}^2)}{[\gamma^4-2\gamma^2+1](\hat{P}^4+1)+4[\gamma^4-1](\hat{P}^3+\hat{P})+(6\gamma^4+4\gamma^2+6)\hat{P}^2}-1\right]\frac{\int_0^{2\pi}\phi^2\sin^2(\theta)\,\mathrm{d}\theta}{4\pi(\gamma-1)}\\
&= \left.\frac{\Delta S}{R}\right|_{\text{eq.}}+\left[\frac{8\gamma^2([\gamma^2-1]\hat{P}^3+[\gamma^2+1]\hat{P}^2)}{[\gamma^4-2\gamma^2+1](\hat{P}^4+1)+4[\gamma^4-1](\hat{P}^3+\hat{P})+(6\gamma^4+4\gamma^2+6)\hat{P}^2}-1\right]\frac{\phi^2}{4(\gamma-1)}\\
&= \left.\frac{\Delta S}{R}\right|_{\text{eq.}}+\left[\frac{4\gamma^2(\gamma-1)M_1^6-4\gamma(\gamma^2-3\gamma+1)M_1^4+(\gamma-1)(\gamma^2-6\gamma+1)M_1^2+(\gamma-1)}{\gamma(\gamma-1)^2M_1^8=4^*\gamma(\gamma-1)M_1^6+4\gamma M_1^4}-1\right]\frac{\mu^2}{4(\gamma-1)}\\
&= \left.\frac{\Delta S}{R}\right|_{\text{eq.}}+G_{\Delta,M}\mu^2
\end{aligned}
\tag{19}
$$

where the steady-state value of $\Delta s/R$ is the value at the steady-state pressure. At $\gamma = 7/5$,

$$
\begin{aligned}
G_{\Delta s,P} &= \frac{2940\hat{P}^3+9065\hat{P}^2}{288(\hat{P}^4+1)+3552(\hat{P}^3+\hat{P})+11528\hat{P}^2}-\frac{5}{8}\\
&= \frac{10.638(0.960\hat{P}^3+2.960\hat{P}^2)}{\hat{P}^4+1+12.333\hat{P}^3+\hat{P}+40.028\hat{P}^2}-0.625\\
&= \frac{490M_1^6+1085M_1^4-340M_1^2+25}{56M_1^8+560M_1^6+1400M_1^4}-\frac{5}{8}\\
&= \frac{2.790\left(3.136M_1^6+6.944M_1^4-2.176M_1^2+0.160\right)}{M_1^8+10M_1^6+25M_1^4}-0.625
\end{aligned}
\tag{20}
$$

This also has a zero value $G_{\Delta s,p} = 0$ at $M_1 = 2.198$. Below that Mach number, $G_{\Delta s,p}$ is positive, and a periodically oscillating shock has more entropy rise than the steady-state shockwave.

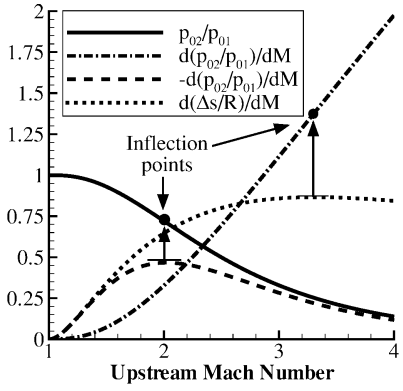


**Fig. 6 Shock total pressure ratio and entropy jump and derivatives with respect to upstream Mach number at $\gamma = 1.4$. Zero-slope points on the derivative curves correspond to inflection points, which determine the unsteady behavior.**

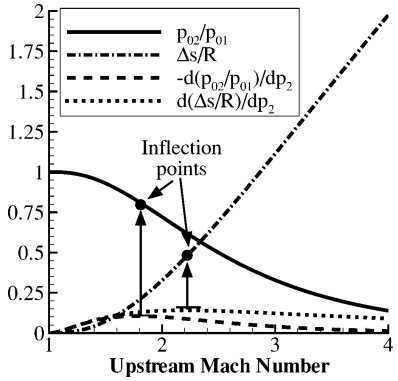


**Fig. 7 Shock total pressure ratio and entropy jump and derivatives with respect to downstream static pressure at $\gamma = 1.4$. Zero-slope points on the derivative curves correspond to inflection points, which determine the unsteady behavior.**

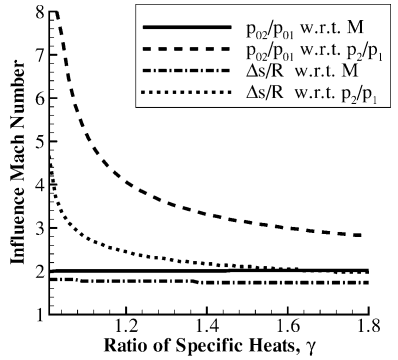


**Fig. 8 Inflection points for entropy and total pressure with respect to Mach number and static pressure, as a function of gamma. The inflection Mach number for entropy is very sensitive to the value of $\gamma$.**

have inflection points, corresponding to the zero-slope points in the first derivative. A symmetric disturbance in Mach number centered at the inflection point will yield no net change in the dependent quantity. At any other point on the curve, a symmetric disturbance will yield a net change, as the gain or loss on one side of the steady-state point will be of a different magnitude than the gain or loss on the other side. Figure 7 presents the inflection points with respect to static-pressure ratio as a function of Mach number, also at $\gamma = 1.4$. Note that the Mach numbers at which these points are located are different than those of Fig. 5, but the qualitative behavior is similar. Figure 8 is the locus of entropy jump inflection points as a function of $\gamma$.

This result can be obtained by taking the second derivatives of Eqs. (1) and (2), respectively.

$$\frac{\mathrm{d}^2[p_{02}/p_{01}]}{\mathrm{d}M_1^2} = \left[\frac{([\gamma+1]M_1)^2}{\left(2\gamma[\gamma-1]M_1^4 - [\gamma^2-6\gamma+1]M_1^2 - 2[\gamma-1]\right)}\right]^{\gamma/(\gamma-1)} \times \left[\frac{4\gamma\left(M_1^2-1\right)\left(2\gamma M_1^6 - [9\gamma-1]M_1^4 + 3[\gamma-1]M_1^2 - 2\right)}{\left(2\gamma[\gamma^2-2\gamma+1]M_1^8 - [\gamma^3-11\gamma^2+11\gamma-1]M_1^6 - 4[\gamma^2-4\gamma+1]M_1^4 - 4[\gamma-1]M_1^2\right)}\right] \tag{21}$$

Equation (21) has an inflection point at values of $M_1$ for which

$$2\gamma M_1^6 - [9\gamma-1]M_1^4 + 3[\gamma-1]M_1^2 - 2 = 0 \tag{22}$$

This is the same zero as in Eq. (8). Solving for the inflection point of the entropy jump, the second derivative is

$$\frac{1}{R}\frac{\mathrm{d}^2\Delta s}{\mathrm{d}M_1^2} = \frac{-8\gamma^2[\gamma-1]M_1^8 + 4\gamma[11\gamma^2-6\gamma-1]M_1^6 - 16\gamma[3\gamma^2-4\gamma-1]M_1^4 + 4\gamma[3\gamma^2-14\gamma-1]M_1^2 + 8\gamma[\gamma-1]}{4\gamma^2[\gamma-1]M_1^{10} - 4\gamma[\gamma^3-7\gamma^2+7\gamma-1]M_1^8 + [\gamma^4-20\gamma^3+54\gamma^2-20\gamma+1]M_1^6 + [4\gamma^2-2\gamma+1]M_1^2} \tag{23}$$

which is zero at the Mach number that satisfies

$$2[\gamma-1]\left(\gamma M_1^6+1\right) - [9\gamma^2-4\gamma-1]M_1^4 + [3\gamma^2-4\gamma-1]M_1^2 = 0 \tag{24}$$

This is the same inflection point that satisfies the integral solution of Eq. (12).

### D. Absolute-Frame Total Pressure Ratio

The inflection point in total pressure has similar behavior to that of the entropy, but the total pressure changes measured in the moving shock frame of reference will not be equal to the total pressure changes in the absolute frame. The absolute-frame total pressure ratio is of interest because it represents the actual losses experienced by an inlet or a nozzle as a result of unsteady effects. Note that with a moving shock the familiar relationship between total pressure and entropy $\Delta s = -R\,\ln(p_{0,2}/p_{0,1})$ does not hold because total temperature is not constant in the moving frame. The concepts of total conditions are still valid under the quasi-steady assumption, but would of course lose meaning in a truly unsteady flow.

To find the total pressure ratio in the absolute frame, we shall first define an instantaneous transformation function $f$ such that

$$f \equiv \left.\frac{p_{0,2}}{p_{0,1}}\right|_{\mathrm{abs}} \Big/ \left.\frac{p_{0,2}}{p_{0,1}}\right|_{\mathrm{shock}} \tag{25}$$

This transformation function is determined from the isentropic relations corrected for the changing Mach number in the moving frame. If the shock is moving at an instantaneous Mach number $M_1$, which produces a downstream Mach number $M_2$, solving for the transformation function depends on relating the upstream and downstream Mach numbers in the absolute frame to the shock-frame upstream Mach number:

$$f = \left(\left\{\frac{1+[(\gamma-1)/2]M_{2,\mathrm{abs}}^2}{1+[(\gamma-1)/2]M_2^2}\right\}\left\{\frac{1+[(\gamma-1)/2]M_1^2}{1+[(\gamma-1)/2]M_{1,\mathrm{abs}}^2}\right\}\right)^{\gamma/(\gamma-1)} \tag{26}$$

From the shock relations, in the shock frame of reference the downstream Mach number can be written explicitly in terms of upstream Mach number $M_2 = \sqrt{[(2+[\gamma-1]M_1^2)/(\gamma M_1^2 - [\gamma-1])]}$. By assumption, the upstream absolute-frame Mach number is constant, and the downstream absolute-frame Mach number is, from continuity arguments, equal to $M_{2,\mathrm{abs}} = M_2(M_{1,\mathrm{abs}}/M_1)$.

Total pressure can be translated from the moving frame to the absolute frame by the transformation function, Eq. (26). However, because the real quantity of interest is the second derivative of pressure, we apply the chain rule:

$$\frac{\mathrm{d}^2(p_{02}/p_{01})_{\mathrm{abs}}}{\mathrm{d}M_1^2} = f\frac{\mathrm{d}^2(p_{02}/p_{01})_{\mathrm{shock}}}{\mathrm{d}M_1^2} + 2\frac{\mathrm{d}(p_{02}/p_{01})_{\mathrm{shock}}}{\mathrm{d}M_1}\frac{\mathrm{d}f}{\mathrm{d}M_1} + \frac{\mathrm{d}^2 f}{\mathrm{d}M_1^2}\left(\frac{p_{02}}{p_{01}}\right)_{\mathrm{shock}} \tag{27}$$

In accordance with the earlier analysis, the quantities of interest are the derivatives at the exact instant the shock wave is perturbed, that is, where the mean Mach number of the perturbation is instantaneously equal to the Mach number in the absolute frame.

### E. Convected Quantities

In one oscillation cycle, the convected mass flux across the shock will be time varying, and this could produce higher-order variations in the mass-weighted downstream entropy. In the absolute frame, mass flux is constant, but in the moving shock frame an increase in the upstream Mach number corresponds directly with an increase in velocity, which for constant upstream density means an increase in mass flux across the shock. In the absolute frame mass flux is conserved as well, but the product of variation in mass flux and entropy change can produce higher-order differences in the convected entropy. The change in convected entropy flux, normalized to upstream density and speed of sound, is

$$\frac{1}{\rho_1 a_1 R}\frac{\mathrm{d}(\rho u \Delta s)_2}{\mathrm{d}M_1} = \left[1-\frac{\rho_2}{\rho_1}\right]\frac{\Delta s}{R} + M_1\frac{\mathrm{d}(\Delta s/R)}{\mathrm{d}M_1}\qquad \frac{1}{\rho_1 a_1 R}\frac{\mathrm{d}^2(\rho u \Delta s)_2}{\mathrm{d}M_1^2} = M_1\frac{\mathrm{d}^2(\Delta s/R)}{\mathrm{d}M_1^2} + \left[2-\frac{\rho_2}{\rho_1}\right]\frac{\mathrm{d}(\Delta s/R)}{\mathrm{d}M_1} - \frac{\Delta s}{R}\frac{\mathrm{d}(\rho_2/\rho_1)}{\mathrm{d}M_1}$$

$$= \frac{4[\gamma+1]\left(2\gamma M_1^3-[\gamma-1]M_1\right)^2(\Delta s/R) + 8\gamma\left[2\gamma M_1^8-(3\gamma^2+9\gamma-2)M_1^6+(4\gamma^2+9\gamma-7)M_1^4-(\gamma^2+3\gamma-6)M_1^2+[\gamma-1]\right]}{-4(\gamma^2-1)^2\left[\gamma^2 M_1^9+M_1\right]+4(\gamma^3-7\gamma^2+7\gamma-1)\left[\gamma M_1^7-M_1^3\right]-(\gamma^4-20\gamma^3+54\gamma^2-20\gamma+1)M_1^5} \tag{30}$$

Taking the derivatives of $f$, and evaluating them at $M_{1,\mathrm{abs}} = M_1$,

$$\left.\frac{\mathrm{d}f}{\mathrm{d}M_1}\right|_{M_{1,\mathrm{abs}}=M_1} = 4\frac{\gamma\left[M_1^4\gamma-2(\gamma-1)M_1^2-2\right]}{\left(2+M_1^2[\gamma-1]\right)(\gamma^2-1)M_1^3}$$

$$\left.\frac{\mathrm{d}^2 f}{\mathrm{d}M_1^2}\right|_{M_{1,\mathrm{abs}}=M_1} = \frac{4\gamma}{\left[\left(2+[\gamma-1]M_1^2\right)(\gamma^2+1)M_1^3\right]^2}$$

$$\begin{bmatrix}(\gamma^4-\gamma^3+5\gamma^2-\gamma)M_1^8+(6[\gamma^4+\gamma+1]-10\gamma^3-4\gamma^2)M_1^6\\+(26\gamma^3-10[\gamma^2+1]-22\gamma)M_1^4+(28\gamma^2+32\gamma-4)M_1^2+16\end{bmatrix} \tag{28}$$

Substituting back into Eq. (27), this gives

As with the derivative of specific entropy, the first derivative changes from positive to negative as Mach number increases, and the second derivative has a zero at Mach 1.989, occurring at a somewhat smaller Mach number than that of the zero for downstream specific entropy.

The integrated cycle of convected entropy can also be computed as the product of $\rho u s$ through one cycle. If the shock is perturbed about an equilibirum point, as in Eq. (4), such that the upstream velocity is written as $u_1 = a_1\hat{M}[1+\varepsilon(t)]$, the total flux of entropy convected downstream can be written as

$$\rho_2(u_2-\hat{M}a_1\varepsilon)[\Delta s+s_1] = \rho_1 a_1\hat{M}\left[1+\varepsilon\left(1-\frac{\rho_2}{\rho_1}\right)\right][\Delta s+s_1]$$

$$= \rho_1 a_1\hat{M}\left\{1+\varepsilon\left[1-\frac{(\gamma+1)\hat{M}^2(1+\varepsilon)^2}{(\gamma-1)\hat{M}^2(1+\varepsilon)^2+2}\right]\right\}[\Delta s+s_1] \tag{31}$$

$$\frac{\mathrm{d}^2(p_{02}/p_{p01})_{\mathrm{abs}}}{\mathrm{d}M_1^2} = \left\{\begin{array}{l}\left[\dfrac{([\gamma+1]M_1)^2}{\left(2\gamma[\gamma-1]M_1^4-[\gamma^2-6\gamma+1]M_1^2-2[\gamma-1]\right)}\right]^{\gamma/(\gamma-1)}\\ \times\dfrac{4\gamma\left(M_1^2-1\right)\left(2\gamma M_1^6-[9\gamma-1]M_1^4+3[\gamma-1]M_1^2-2\right)}{\left(2\gamma[\gamma^2-2\gamma+1]M_1^8-[\gamma^3-11\gamma^2+11\gamma-1]M_1^6-4[\gamma^2-4\gamma+1]M_1^4-4[\gamma-1]M_1^2\right)}\end{array}\right\}$$

$$+\left[\begin{array}{l}8\dfrac{\gamma\left[M_1^4\gamma-2(\gamma-1)M_1^2-2\right]}{\left(2+M_1^2[\gamma-1]\right)(\gamma^2-1)M_1^3}\gamma M_1\left[\dfrac{1+2\gamma\left(M_1^2-1\right)}{\gamma+1}\right]^{-1/(\gamma-1)}\left[\dfrac{(\gamma-1)M_1^2+2}{(\gamma+1)M_1^2}\right]^{-\gamma/(\gamma-1)}\\ \times\left(\dfrac{-4}{(\gamma^2-1)\left[1+2\gamma\left(M_1^2-1\right)/(\gamma+1)\right]}-\dfrac{\left\{2(\gamma-1)/M_1(\gamma+1)-2\left[(\gamma-1)M_1^2+2\right]/(\gamma+1)M_1^3\right\}(\gamma+1)M_1}{(\gamma-1)\left([\gamma-1]M_1^2+2\right)}\right)\end{array}\right]$$

$$+\left(\begin{array}{l}\left[1+\dfrac{2\gamma}{\gamma+1}\left(M_1^2-1\right)\right]^{-1/(\gamma-1)}\left\{\dfrac{\left[\begin{array}{l}(\gamma^4-\gamma^3+5\gamma^2-\gamma)M_1^8+(6[\gamma^4+\gamma+1]-10\gamma^3-4\gamma^2)M_1^6\\+(26\gamma^3-10[\gamma^2+1]-22\gamma)M_1^4+(28\gamma^2+32\gamma-4)M_1^2+16\end{array}\right]}{\left[\left(2+[\gamma-1]M_1^2\right)(\gamma^2+1)M_1^3\right]^2}\right\}\\ \times\left[\dfrac{(\gamma-1)M_1^2+2}{(\gamma+1)M_1^2}\right]^{-\gamma/(\gamma-1)}4\gamma\left\{1+\dfrac{\gamma[\gamma+1]\left(M_1^2-1\right)\left(2\gamma M_1^6-[9\gamma-1]M_1^4+3[\gamma-1]M_1^2-2\right)}{\left[\left([\gamma-1]M_1^2+2\right)\left(2\gamma M_1^2-[\gamma-1]\right)\right]}\mu^2\right\}\end{array}\right) \tag{29}$$

A plot of the second derivative of total pressure in the absolute frame of reference, Eq. (29) is shown in Fig. 9, along with the second derivative in the shock frame and the entropy rise. Note that there is no inflection point for the absolute frame; unsteadiness always yields downstream time-averaged total pressure, which is lower than the steady flow case.

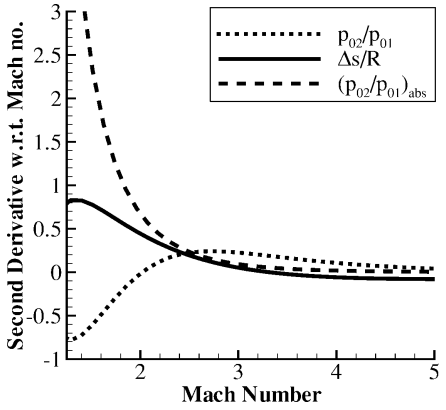


**Fig. 9 Second derivative of entropy and total pressure ratio with respect to Mach number.**

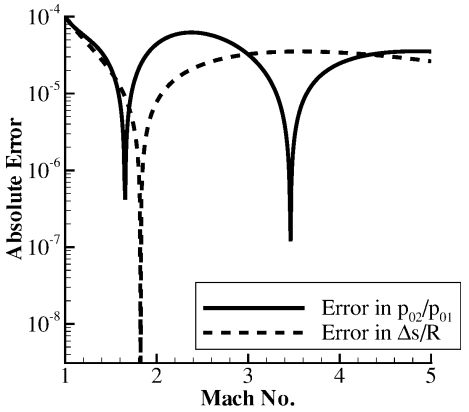


**Fig. 10 Difference between calculated and computed total pressure ratio and entropy drop over a Mach oscillation cycle (1000 time points, 500 Mach points).**

Substituting for $\Delta s/R$ from Eq. (10), writing $\varepsilon = \mu \sin \omega t$, and expanding and integrating through one cycle,

$$\left.\frac{\rho u(\Delta s/R)}{\rho_1 u_1}\right|_{\text{avg.}} \cong \left.\frac{\Delta s}{R}\right|_{\text{equil}} + \left\{ \left. -\frac{2[\gamma+1]M_1^2}{\left(2+[\gamma-1]M_1^2\right)^2}\frac{\Delta s}{R}\right|_{\text{equil}} + \frac{4\gamma\left(1-M_1^2\right)^3}{\left(2+[\gamma-1]M_1^2\right)^2\left(2\gamma M_1^2-[\gamma-1]\right)} - \left(M_1^2-1\right) - \frac{2[\gamma-1]\left(\gamma M_1^6+1\right)-[9\gamma^2-4\gamma-1]M_1^4+3[\gamma^2-4\gamma-1]M_1^2}{4\gamma\left[\left([\gamma-1]M_1^2+2\right)\left(2\gamma M_1^2-[\gamma-1]\right)\right]^2} \right\}\mu^2 \tag{32}$$

where once again, odd terms in $\varepsilon$ cancel out in each cycle, leaving only terms in $\varepsilon^2$. Qualitative behavior is similar to that of the time average of specific entropy jump.

## III. Comparison of Analytical Results and Numerical Solution

To confirm the validity of the perturbation analysis presented earlier in this paper, the derived approximations for various time-averaged properties are compared to the results of a numerical solution in which either Mach number or static-pressure ratio are driven through one oscillation cycle, and the appropriate properties are time-averaged over each point in the cycle.

Figure 10 shows the absolute difference between the total pressure ratio and entropy drop, computationally averaged over a 10% variation in Mach number for Eqs. (7) and (11). Figure 11 shows the absolute difference between the same properties, computationally averaged over a 10% variation in static pressure for Eqs. (16) and (19).

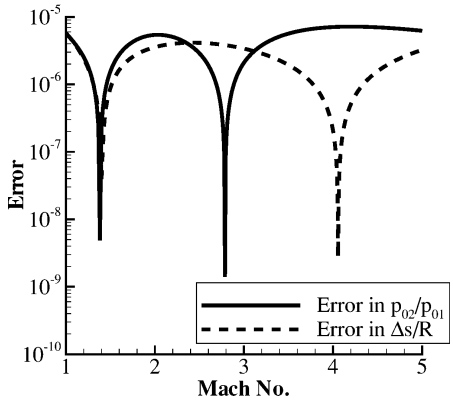


**Fig. 11 Difference between calculated and computed total pressure ratio and entropy drop over a pressure oscillation cycle (1000 time points, 500 Mach points).**

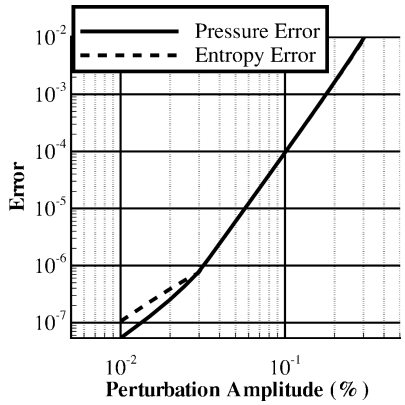


**Fig. 12 Maximum absolute difference between calculated and computed total pressure ratio and entropy drop as a function of Mach-number perturbation amplitude (1000 time points, 500 Mach points).**

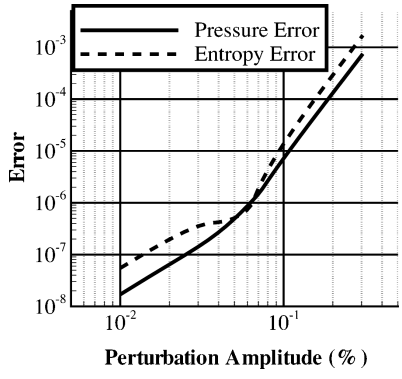


**Fig. 13 Maximum absolute difference between calculated and computed total pressure ratio and entropy drop as a function of static-pressure ratio perturbation amplitude (1000 time points, 500 Mach points).**

Finally, Figs. 12 and 13 show the maximum error as a function of Mach and static-pressure perturbation amplitude, respectively. Here, the error appears be about fourth order for both curves when plotted on log-log axes, which is to be expected given that the third-order and higher terms were discarded, and the third-order terms, being odd, integrate to zero. The knee in the curves is indicative of the point where machine error of the computation code becomes comparable to the error of the approximations.

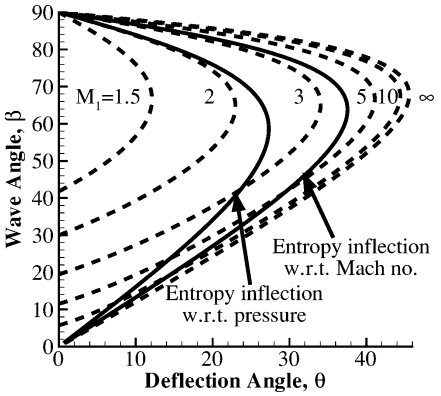


**Fig. 14 $\theta$-$\beta$-Mach diagram showing the region where an unsteady shock will have an entropy rise, which is lower than steady state, and the region where it is higher.**

## IV. Application to Oblique Shock Waves

Thus far, this analysis has only been applied to normal shock waves. It can be readily extended to two-dimensional oblique shock waves because the same governing equations apply to both oblique and normal shocks, except that for an oblique shock,

$$M_1 = M_{n,1}/\sin\beta \tag{33}$$

In two-dimensional oblique flow, the time-averaged unsteady behavior is a function of both upstream Mach number and shock-wave deflection angle $\beta$ following the familiar $\theta$–$\beta$–$M$ equation,

$$\tan\theta = 2\cot\beta\frac{M_1^2\sin^2\beta - 1}{M_1^2(\gamma + \cos 2\beta) + 2} \tag{34}$$

For example, with a Mach 10 upstream, the entropy inflection point will occur at a shock angle near $\beta = 13$ deg, which corresponds to a wedge angle, $\theta = 8.6$ deg. Thus, for an engine inlet designed for Mach 10 operation, an inlet wedge angle of 10 deg will produce an inlet shock in which unsteadiness produces less time-averaged entropy than steady flow, resulting in an inherently unsteady inlet. However, an inlet wedge angle of 5 deg will result in more entropy rise with unsteady flow, likely yielding an inherently steady inlet. The regions of higher and lower entropy can be mapped onto a $\theta$–$\beta$–$M$ diagram, as shown in Fig. 14.

The two forms of unsteadiness indicated here would manifest themselves as oscillations in $\beta$ such that the normal Mach number or the static-pressure ratio, respectively, would vary. An oblique shock could include other modes of oscillation, such as if $\beta$ or the freestream Mach number (rather than the normal Mach number) varied sinusoidally. Also, an oblique wave could oscillate in the $x$ direction, rather than angularly. Numerous studies have been performed on the stability of oblique shocks,[7–10] as well as their oscillations characteristics.[8,12]

## V. Implications

Both analytical and numerical solutions of the perturbed quasi-steady shock relations demonstrate that the conditions across a sinusoidally perturbed shock wave differ from conditions across a steady shock wave in a manner that is dependent on the value of the normal Mach number. Both the magnitude and sign of these differences are affected, and crossover points in the behavior occur at Mach values that can be experienced by a hypersonic inlet. For a flow at low supersonic Mach number, unsteadiness will generally increase the time average of entropy rise as flow crosses a normal shock.

In terms of practical application to supersonic vehicles, because unsteadiness always yields a drop in time-averaged total pressure, if the minimum entropy production principle holds the entropy behavior across the shock should generally lead to improved supersonic inlet performance, but should penalize a hypersonic inlet. This analysis further suggests that an inlet which is passing through a range of Mach numbers can begin supersonic operation with a tendency towards steady shock flow, but will be more likely to behave in an unsteady manner at hypersonic flight conditions. This in turn will translate directly into lost propulsive work and reduced specific impulse.

Note that these results depend on the applicability of the quasi-steady assumption; for extremely high relative perturbation frequencies, measured in comparison to the inverse of flow passage time, very different time-dependent behavior can be observed. In the extreme case of sufficiently high frequency such that positive and negative disturbances effectively cancel each other downstream, shock unsteadiness can have little impact on the downstream inviscid thermodynamic properties. Also, because the quasi-steady assumption includes continuity of mass flow across the shock, several terms in the entropy derivative drop out, which can contribute significant entropy production in a higher-order analysis. Finally, conclusions that might be drawn on the tendency of shocks to be either steady or unsteady based on the changes in entropy production will also depend on the ultimate applicability of the minimum entropy production principle, which at this writing is still somewhat speculative.

A realistic inlet will almost certainly have multiple shock waves, and these will in turn complicate the effect of unsteadiness on downstream conditions. For instance, if unsteadiness in the primary shock of a hypersonic inlet leads to an entropy decrease (compared to the steady state), it might be that subsequent shock waves at lower Mach numbers actually increase the overall entropy. This would clearly affect the applicability of the minimum entropy production principle, and the effect of each shock wave would have to be considered in turn. The principle of minimum entropy production, if applicable, would also have to be employed across the entire shock system, which could be quite complicated. This is less likely to be true for a compressor blade or turbine blade passage. Shock-boundary-layer effects could further complicate these results.

## VI. Conclusions

The effects of an imposed perturbation onto a normal shock wave have been explored, using both analytical and computational methods. Because of the nonlinearity of the governing equations, below a given freestream Mach number (i.e., the Mach number about which the shock is perturbed) a stationary wave will produce less entropy than a wave that has a periodically varying Mach number. Above this Mach number, the reverse is true. There is a second critical Mach number, smaller than the first, below which the total pressure losses for a stationary shock will also be smaller than for a moving shock. This means that there is a small range of Mach numbers for which oscillations of the shock will result in lower total pressure losses, but increased entropy production. A similar analysis can be performed by perturbing the pressure ratio across the shock. Such an analysis results in two more critical Mach numbers, lower than their analogous quantities in the Mach-perturbed case, for which the same trends are applicable.

The critical Mach numbers have been identified for the change in net time-averaged response. These are dependent only on the ratio of specific heats of the flow and can be found by either computationally perturbing the equations, and searching for changeovers, or by differentiating the mathematically perturbed Rankine–Hugoniot equations and truncating the solutions to second order. Both methods produce similar results. Overall, when the total pressure ratio across a quasi-steady shock is calculated in the absolute frame of reference, as would be relevant for application to a supersonic inlet or combustor, oscillation will always cause an increase in total pressure losses across the shock. This in turn means that unsteady shocks should always reduce the useful work available for propulsion, as compared to the steady-state solution, regardless of supersonic upstream Mach number.

## Acknowledgments

Portions of this work have been supported under NASA Grant NAGw-11796 and the by the Space Vehicle Technology Institute under Grant NCC3-989 jointly funded by NASA and U.S. Department of Defense within the NASA Constellation University

Institutes Project, with Claudia Meyer as technical monitor, with John Schmisseur of the Air Force Office of Scientific Research, to whom appreciation is expressed.

## References

[1]Lewis, M. J., Surline, Y., and Anderson, J. D., "An Analytical and Computational Study of Unsteady Shock Motion on Hypersonic Forebodies," *Journal of Aircraft*, Vol. 28, No. 8, 1991, pp. 532–539.

[2]Ng, W. F., and Epstein, A. H., "Unsteady Losses in Transonic Compressors," *Journal of Engineering for Gas Turbines and Power*, Vol. 107, No. 2, 1985, pp. 345–353.

[3]Handa, T., Masuda, M., and Matsuo, K., "Mechanism of Shock Wave Oscillation in Transonic Diffusers," *AIAA Journal*, Vol. 41, No. 1, 2003, pp. 64–70.

[4]Berthouze, P., and Bur, R., "Experimental Investigation of the Response of a Transonic Shock-Wave to Downstream Perturbations," AIAA Paper 2001-3295, July 2001.

[5]Bogar, T. J., Sajben, M., and Kroutil, J. C., "Characteristic Frequencies of Transonic Diffuser Flow Oscillations," *AIAA Journal*, Vol. 21, No. 9, 1983, pp. 1232–1240.

[6]Culick, F. E. C., and Rogers, T., "The Response of Normal Shocks in Diffusers," *AIAA Journal*, Vol. 21, No. 10, 1983, pp. 1382–1390.

[7]Carrier, G. F., "On the Stability of the Supersonic Flows Past a Wedge," *Quarterly of Applied Mathematics*, Vol. 6, No. 4, pp. 367–378.

[8]Henderson, L. F., and Atkinson, J. D., "Multi-Valued Solutions of Steady-State Supersonic Flow. Part 1. Linear Analysis," *Journal of Fluid Mechanics*, Vol. 75, Pt. 4, 1976, pp. 751–764.

[9]Rusanov, V. V., and Sharakshanae, A. A., "On the Non-Uniqueness of the Solution of the Problem on Steady Flow About the Plane Wedge and Circular Cone," *Computers and Fluids*, Vol. 8, No. 2, 1979, pp. 243–250.

[10]Salas, M. D., and Morgan, B. D., "Stability of Shock Waves Attached to Wedges and Cones," *AIAA Journal*, Vol. 21, No. 12, 1983, pp. 1611–1617.

[11]Carrier, G. F., "The Oscillating Wedge in a Supersonic Stream," *Journal of the Aeronautical Sciences*, Vol. 16, March 1949, pp. 150–152.

[12]Emanuel, G., and Yi, T. H., "Unsteady Oblique Shock Waves," *Shock Waves*, Vol. 10, No. 2, 2000, pp. 113–117.

[13]Mullagiri, S., Segal, C., and Hubner, P. J., "Oscillating Flows in a Model Pulse Detonation Engine Inlet," *AIAA Journal*, Vol. 41, No. 2, 2003, pp. 324–326.

[14]Mullagiri, S., and Segal, C., "Oscillating Flows in Inlets of Pulse Detonation Engines," AIAA Paper 2001-0669, Jan. 2001.

[15]Nori, V., Lerma, N., and Segal, C., "Oscillatings Flows in Inlets for Pulsed Detonation Engines," AIAA Paper 2003-886, Jan. 2003.

[16]Gustavsson, J., Nori, V., and Segal, C., "Inlet/Engine Interactions in an Axisymmetric Pulse Detonation Engine System," *Journal of Propulsion and Power*, Vol. 19, No. 2, 2003, pp. 282–286.

[17]Li, H., and Ben-Dor, G., "Applications of the Principle of Minimum Entropy Production to Shock Wave Reflections. Part I. Steady Flows," *Journal of Applied Physics*, Vol. 80, No. 4, 1996, pp. 2027–2037.

[18]Li, H., and Ben-Dor, G., "Applications of the Principle of Minimum Entropy Production to Shock Wave Reflections. Part II. Pseudosteady Flows," *Journal of Applied Physics*, Vol. 80, No. 4, 1996, pp. 2038–2048.

[19]Lewis, M. J., "Designing Hypersonic Inlets for Bow Shock Location Control," *Journal of Propulsion and Power*, Vol. 9, No. 2, 1993, pp. 313–321.

[20]Lind, C., and Lewis, M. J., "Unsteady Characteristics of a Hypersonic Type IV Shock Interaction," *Journal of Aircraft*, Vol. 32, No. 6, 1995, pp. 1286–1293.

[21]Hurrell, H., "Analysis of Shock Motion in Ducts During Disturbances in Downstream Pressure," NACA TN 4090, 1957.